[논 문] 한국재료학회지
Kor. J. Mater. Res.
Vol. 20, No. 4 (2010)

DOI: 10.3740/MRSK.2010.20.4.228

Preparation of Different Fe Containing TiO_2 Photocatalysts and Comparison of Their Photocatalytic Activity

Ze-Da Meng, Kan Zhang and Won-Chun Oh†

Department of Advanced Materials & Science Engineering, Hanseo University, Seosan-si, Chungnam-do 356-706, Korea

(Received March 27, 2010 : Received in revised form April 17, 2010 : Accepted April 18, 2010)

Abstract In this paper, Fe-TiO_2 and Fe-fullerene/TiO_2 composite photocatalysts were prepared with titanium (IV) n-butoxide (TNB) by a sol-gel method. TiO_2, Fe-TiO_2 and Fe-fullerene/TiO_2 were characterized by scanning electron microscopy (SEM), Transmission electron microscope (TEM), specific surface area (BET), X-ray diffraction analysis (XRD) and energy dispersive X-ray spectroscopy (EDX). The photocatalytic activities were evaluated by the photocatalytic oxidation of methylene blue (MB) solution. XRD patterns of the composites showed that the photocatalyst composite contained a typical single and clear anatase phase. The surface properties shown by SEM presented a characterization of the texture on Fe-fullerene/TiO_2 composites and showed a homogenous composition in the particles for the titanium sources used. The EDX spectra for the elemental identification showed the presence of O, C and Ti elements. Moreover, peaks of the Fe element were observed in the Fe-TiO_2 and Fe-fullerene/TiO_2 composites. The degradation of MB solution by UV-light irradiation in the presence of photocatalyst compounds was investigated in complete darkness. The degradation of MB concentration in aqueous solution occurred via three kinds of physical phenomena: quantum efficiency of the fullerene; organo-metallic reaction of the Fe compound; and decomposition of TiO_2. The degradation rate of the methylene blue solution increased when using Fe-fullerene/TiO_2 compounds.

Key words Fe-Fullerene/TiO_2, UV-light, SEM, TEM, methylene blue.

1. Introduction

The photocatalytic process with using TiO_2 photocatalyst is very promising for application in the water purification, because many hazardous organic compounds can be decomposed and mineralized by the proceeding oxidation and reduction processes on TiO_2 surface.[1)] The most commonly tested compounds for decomposition through the photocatalysis are phenols, chlorophenols, pesticides, herbicides, benzenes, alcohols, dyes, pharmaceutics, humic acids, organic acids and others.[1-8)]

Many efforts are focused on the practical application of TiO_2 in the water treatment system. Titania has three different crystalline phases; rutile, anatase and brookite, among which rutile is in thermodynamically stable state while the latter two phases are in metastable state.[9)] Photocatalytic activity of titania may strongly depend on its phase structure, crystallite size, the specific surface areas and pore structure and so on, for example, many studies have confirmed that the anatase phase of titania is the superior photoactalytic materials for air purification, water disinfection, hazardous waste remediation, and water purification.[7,8)]

†Corresponding author
E-Mail : wc_oh@hanseo.ac.kr(W. -C. Oh)

However, the efficiency of the photocatalytic degradation reaction is limited by the high recombination rate of photoinduced electrons and holes. Much effort has been contributed to improve the photocatalytic efficiency of TiO_2 by doping with transition metal ions, surface depositing of noble metal clusters and coupling TiO_2 with other semiconductors.[11-21)] In particular, iron (III)-doped TiO_2 samples have been the object of many papers, including preparation and characterization, spectroscopic features, dynamics of charge transfer trapping and photocatalytic behavior.[22-24)] Iron doping can give some benefits such as retarding the inconvenient recombination reaction, which proceeds after photocatalyst excitation and also can extend the photocatalytic ability of the photocatalyst to the visible region.

Several studies have investigated the derivative media of the fullerenes, due in part to their wide application in photoconductive, photovoltaic, and optical properties.[25-27)] In the new field of material sciences associated with nano-size carbon materials and the chemistry involved in the preparation of nanocarbon derivatives,[28-31)] the interesting, higher nano-size carbon materials have received special attention. Recently, carbon based TiO_2 composites have attracted much attention and have become a very active field of research due to their unique properties and promising applications in pollution management.[32-37)] In

particular, fullerenes (C_{60}) and carbon nanotubes (CNT) have attracted considerable attention as of late owing to their remarkable photoelectrical and mechanical properties,[38] as well as their subsequent composites that possess intrinsic properties as materials exhibiting cooperative and/or synergetic effects.

This study presents the preparation and characterization of Fe-fullerene/TiO_2 composites synthesized by sol-gel method. Structural variations, surface state and photocatalytic performance were investigated, by preparing Fe-fullerene and composites sequentially after oxidation, compare to the pure TiO_2 and Fe-TiO_2 compounds. X-ray diffraction (XRD), scanning electron microscopy (SEM), energy dispersive X-ray (EDX) spectroscopy and Transmission electron microscope (TEM) were used to characterize the new complexes. In order to obtain a novel photocatalyst with appropriate adsorbability and high catalytic, the combination method of semiconductor (TiO_2) particles was adopted and the two composites Fe-TiO_2 and Fe-Fullerene/TiO_2 were prepared. This paper compares the degradation rate between these three catalysts. The results showed that the prepared composite Fe-fullerene/TiO_2 not only had a satisfactory adsorbability but also exhibited a comparatively high catalytic activity.

2. Experimental Methods

2.1 Materials

Crystalline fullerene [C_{60}] powder of 99.9% purity from TCI (Tokyo Kasei Kogyo Co. Ltd., Japan) was used as the carbon matrix. Benzene and ethyl alcohol were purchased as reagent-grade from Duksan Pure Chemical Co (Korea) and Daejung Chemical Co. (Korea) and used without further purification unless otherwise stated. Ferric nitrate [$Fe(NO_3)_3$] as a iron source for the synthesis of the Fe-fullerene compounds was purchased as reagent-grade from Duksan Pure Chemical Co. (99+%, ACS reagent, Korea).

The titanium (IV) n-butoxide (TNB, $C_{16}H_{36}O_4Ti$) as a titanium source for the preparation of the Fe-fullerene/TiO_2 composites was purchased as reagent-grade from Acros Organics (USA). Methylene blue (MB, $C_{16}H_{18}N_3S.Cl.3H_2O$) was analytical grade and also purchased from Duksan Pure Chemical Co., Ltd.

2.2 Chemical oxidation on the fullerene surface and Fe treated

m-Chloroperbenzoic acid (MCPBA, ca. 1 g) was suspended in 50 ml benzene, followed by the addition of fullerene [C_{60}] (ca. 100 mg). The mixture was then refluxed in an air atmosphere and stirred for 6h. The solvent was subsequently dried at the boiling point of benzene (353.13 K). After completion, the dark brown precipitates were washed with ethyl alcohol and dried at 323 K. Added ferric nitrate solution (0.05 M). This mixture was refluxed in an air atmosphere and stirred at 343 K for 6h using a magnetic stirrer in a vial. After being heat treatment at 773 K for 1h, the Fe-fullerene compounds were formed.

2.3 Preparation of Fe-fullerene/TiO_2 composites

Fe-fullerene was prepared by using pristine concentrations of TNB for the preparation of Fe-fullerene/TiO_2 composites. Fe-fullerene powder was mixed with 3 ml TNB. Then the solution was homogenized under reflux at 343 K for 5h, while being stirred in a vial again. After stirred, the solution transformed into Fe-fullerene/TiO_2 gels, and these gels were heat treatment at 923 K, then Fe-fullerene/TiO_2 composites were produced. After heat treated titanium (IV) n-butoxide (TNB, $C_{16}H_{36}O_4Ti$) at 927K, TiO_2 sample was prepared. Fe-TiO_2 sample was prepared by sol-gel method.

2.4 Characterization of Fe-fullerene/TiO_2 compounds

For the measurements of structural variations, XRD patterns were taken using an X-ray generator (Shimatz XD-D1, Japan) with Cu Kα radiation. An SEM (JSM-5200 JOEL, Japan) was used to observe the surface state and structure of Fe-fullerene/TiO_2 treated with TNB. Energy dispersive X-ray (EDX) spectra were also used for the elemental analysis of the samples. The specific surface area (BET) was determined by N_2 adsorption measurements at 77 K (Monosorb, USA). Transmission electron microscopy (TEM, JEOL, JEM-2010, Japan) were used to observe the surface state and structure of the Fe-fullerene/TiO_2 composites. At acceleration voltage of 200 kV TEM was used to investigate the size and distribution of the titanium particles deposit on the fullerene surface of various samples. TEM specimens were prepared by placing a few drops of the sample solution on a carbon grid.

2.5 Photocatalytic activities

Photocatalytic activities were evaluated by MB degradation in aqueous media under ultraviolet light irradiation. For UV irradiation, the reaction beaker was located axially and held in UV lamp (20 W, 365 nm) box. The lamp was used at a distance of 100 mm from the aqueous solution in the darkness box. The initial MB concentration (C_0) was 1.0×10^{-5} mol/L. 0.05 g photocatalyst (TiO_2, Fe-TiO_2, Fe-fullerene/TiO_2) compounds were added into 50 ml MB solution, placed for 2h in the darkness box. Then suspension was irradiated with UV light as a function of irradiation time. Samples were then withdrawn regularly from the reactor and removal of dispersed powders through a centrifuge. The concentration of MB in the solution was determined as a function of irradiation time.

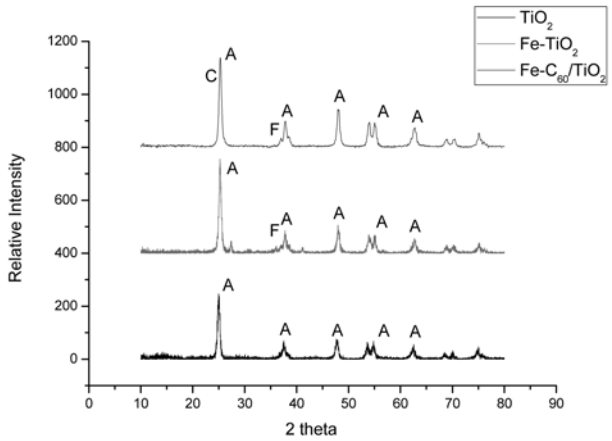

Fig. 1. XRD patterns of photocatalyst composites.

3. Results and Discussion

3.1 Structural analysis

The XRD technique was used to determine the crystallographic structure of the inorganic of the composite. The XRD patterns of the pure TiO_2, Fe-TiO_2 and Fe-fullerene/TiO_2.

From the XRD result of pure TiO_2, shown after heat treatment at 923 K, the major peaks at 25.3, 37.5, 48.0, 53.8, 54.9, and 62.5 were diffractions of (101), (004), (200), (105), (211), and (204) planes of anatase which indicating that the prepared TiO_2 existed in an anatase phase. The results also indicate that the phase transition from TNB to the anatase phase took place at 923 K, with formation of titania crystalline. Anatase phase of titania is the superior photoactalytic materials for air purification, water disinfection, hazardous waste remediation, and water purification.[8,9] The XRD result of Fe doped TiO_2 is clearly denoted the peak of iron oxide, which can also find from EDX image. From XRD image we have not find the peak of Fe_xTiO_y (ferrous titanate) may be the content of iron is so little, only 0.5%~0.9%. The XRD results of the Fe-fullerene/TiO_2 compounds are shown in Fig. 2, C is the characteristic peaks corresponding to the fullerene, A is anatase phase of titania, F is Fe_2O_3. The peak of Fe_2O_3 is weak due to the content of iron is small with the influence of anatase peak. One peak is measured at 2θ values of approximately 25.80° (only one). It's the characteristic peaks corresponding to the fullerene molecular crystal structure. This peak corresponds to d-values of 0.345 nm.[39] Fullerene and one of titanium characteristic peaks are overlap at around 25.0°, so intensity of the peak is increased. Traces of fullerene are detected and a broad diffuse peak in the diffraction pattern is indicative for the presence of amorphous carbon. Moreover, in the curve of samples, we can clearly find the peaks of Fe_2O_3. We could not observe characteristic peaks of Fe-fullerene in the XRD patterns which can find in other paper.[40-42] Maybe Fe_2O_3 was in the surface or inside of fullerene, which was further supported by observation via SEM, EDX and TEM elemental microanalysis of the Fe-fullerene/TiO_2 composite.

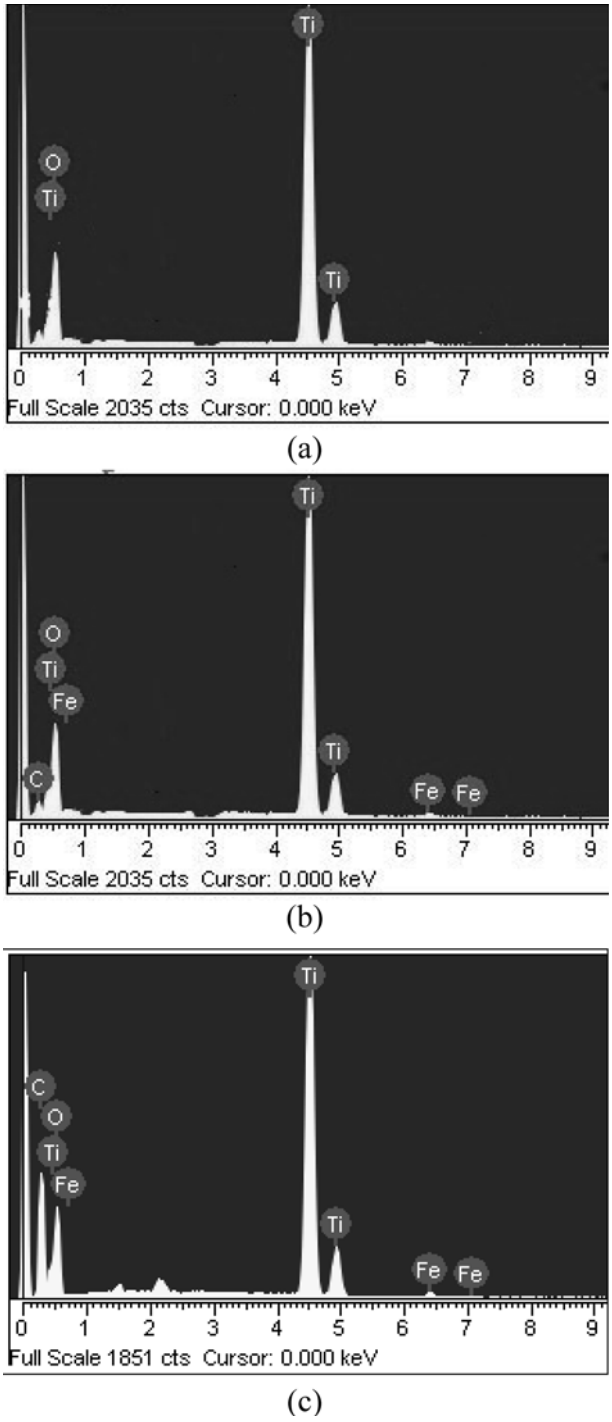

Fig. 2. EDX elemental microanalysis for photocatalyst composites: (a) TiO_2, (b) Fe-TiO_2 and (c) Fe-fullerene/TiO_2.

From Fig. 1 XRD peaks intensity announced that TiO_2 and Fe-TiO_2 has higher crystallinity than Fe-fullerene-

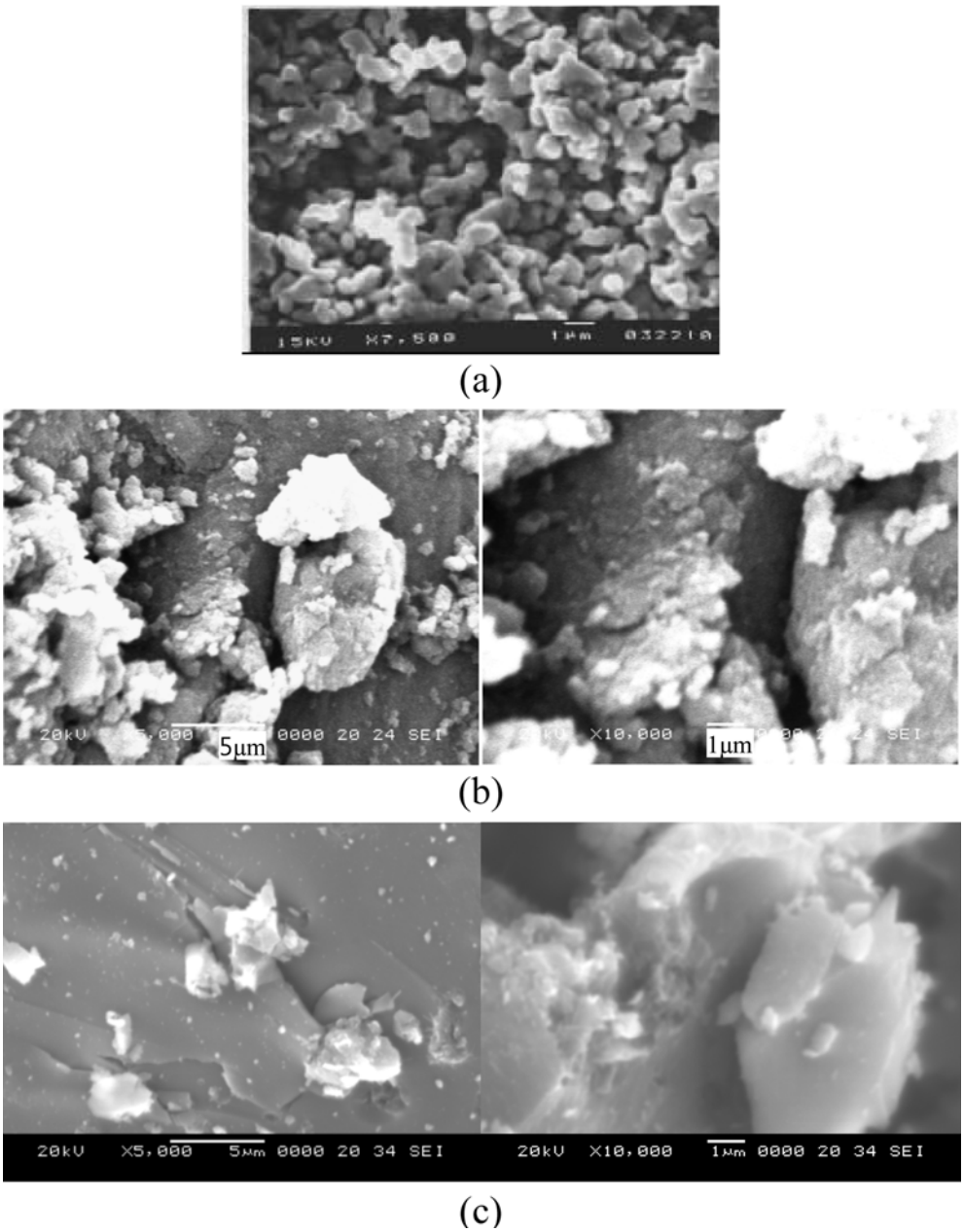

Fig. 3. SEM micrographs of photocatalyst composites: (a) TiO_2, (b) Fe-TiO_2 and (c) Fe-fullerene/TiO_2.

TiO_2. As we know crystallinity is one of major factors determining photocatalytic activity, and has good crystallinity can improve the photocatalytic activity. Although Fe-fullerene-TiO_2's crystallinity is not good, but because of increase specific surface area by fullerene and energy transfer effects such as electron and light of the fullerene, Fe-fullerene-TiO_2 compounds have good photocatalytic activity.

3.2 Elemental analysis

The quantitative microanalysis of C, O, Ti and Fe as major elements for these photocatalyst composites were performed by EDX which were shown in Fig. 3. The EDX results of photocatalyst composite shows the peaks corresponding the C, O, Ti and Fe elements. The numerical result of EDX quantitative microanalysis of these photocatalyst revealed the ratio was shown in Table 2. The spectra show the presence of C, O, and Ti, as major elements, with strong Fe peaks. There are some small impurities, which were considered to introduce into the composites using the fullerene without purification. In the case of the Fe-fullerene/TiO_2 samples, carbon and titanium were present as major elements with small quantities of oxygen in the composite.

Table 1. EDX elemental microanalysis of Fe-fullerene/TiO_2 composites

Sample (wt.%)	C	O	Ti	Fe
TiO_2	3.20	50.36	46.44	0
Fe-TiO_2	4.44	52.09	42.90	0.5
Fe-fullerene/TiO_2	25.01	40.36	33.73	0.90

Table 2. Specific BET surface areas of photocatalyst composites

Sample	S_{BET} (m^2/g)
TiO_2	18.9
Fe-TiO_2	11.2
Fe-fullerene/TiO_2	40.4

3.3 Surface characteristics

The surface characteristics of TiO_2, Fe-TiO_2 and Fe-Fullerene/TiO_2 composites are shown in Fig. 4. SEM micrographs revealed these three different composites derivatives with surface characteristics shown in Fig. 4. It can be clearly seen that the TiO_2 particles prepared at a source temperature of 973 K showed a great distribution of dimension. In Fig. 4(a) is SEM image of TiO_2 at magnification of 7500. The size of TiO_2 particles is about 0.5 um, and the distribution was uniform. In the report of Zhang,[43] a good dispersion of small particles could provide more reactive sites for the reactants than aggregated particles. The image (b) is Fe-TiO_2 compound's SEM image. As shown in the images, the Fe particles were well attached to the surface of the TiO_2 particles, and distribution was uniform.

As shown in image (c), it is Fe-fullerene/TiO_2 composite. The morphological evidences of TiO_2 units onto Fe-fullerene structure which seem to cover the polymer surface. These TiO_2 particles were regularly dispersed on the fullerene surfaces and continuous TiO_2 units was immobilized on almost every grain of fullerene. It is considered that a good dispersion of small particles on the fullerene surface could provide evidence for the existence of more reactive sites for photodecomposition of the dye. But the large clusters with an irregular agglomerate dispersion could not found. Maybe the titanium (IV) n-butoxide (TNB, $C_{16}H_{36}O_4Ti$) as a titanium source have a low proportion. Therefore, the higher photocatalytic activity of the Fe-fullerene/TiO_2 composite might be attributed to the small and nano-sized distribution of titanium complexes including titanium dioxide, the energy sensitizer for improving the quantum efficiency, and an increase of charge transfer of the fullerene.[40]

In Fig. 3, Fe-TiO_2 and Fe-fullerene-TiO_2 is agglomerated, as we know agglomerated is not good for photocatalytic activity, but the addition of Fe and fullerene can reduce the impact.

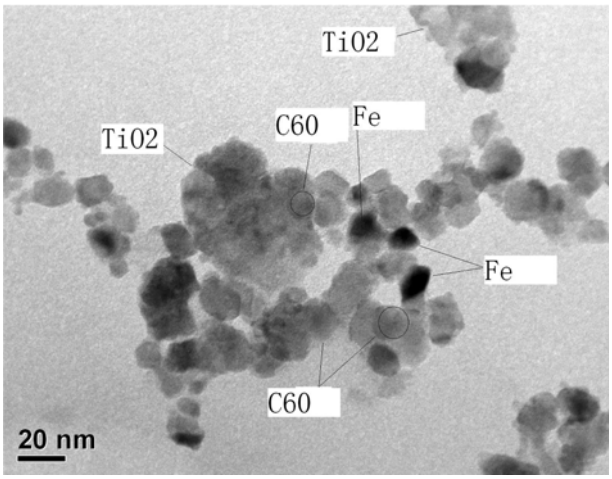

Fig. 4. TEM micrographs of Fe- fullerene /TiO_2 composites.

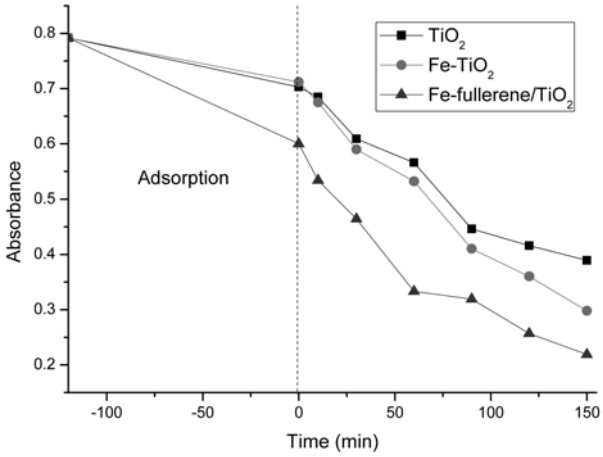

Fig. 5. degradation for MB solution of adsorption and UV irradiation for photocatalyst compounds.

The specific surface area (BET) results were shown in Table 2. Fe-fullerene/TiO_2 particles have the largest surface area which can affect the adsorption reaction. Fullerene has relatively bigger surface area, can enhance the surface area of Fe-fullerene/TiO_2 compounds. The BET value of Fe-TiO_2 is smaller than that of TiO_2, may be Fe doped into TiO_2 particles can decrease the compound's surface area, There are two possible factors resulting in the decrease of specific surface area. One is that the aggregation of smaller crystallites forms smaller pores. The other is that some Fe^{3+} ions of doping probably insert into the pore of pure TiO_2, which also causes pore size to become smaller.

The interfacial region of the Fe-fullerene/TiO_2 compound was investigated by TEM to obtain additional information about the interfacial region of the fullerene crystals and to identify potential reaction products in this domain. From Fig. 5, we can see the large clusters with an irregular agglomerate dispersion of TiO_2. The fullerene

particles were clearly shown from the picture. The light and spherical shape was displayed from Fig. 5 which is fullerene. We also found iron element in TEM image, it was revealed as black point.

3.4 Photocatalytic decomposition of MB

The degradation effects of the MB concentration against the photocatalyst derivative under various time conditions are shown in Fig. 5. From these spectra for the MB solution after photolysis, the relative yields of the photolysis products formed at different irradiation time conditions were shown for the products. The concentration of MB was 1.0×10^{-5} mol/l and the absorbance decreased with increasing irradiation time. This implies that the light transparency of the MB concentration increased greatly by the photocatalytic degradation effect. An effect of the high crystallinity of the anatase phase on photocatalytic degradation of MB has been shown.

Fe-TiO_2 and Fe-fullerene/TiO_2 have higher photoactivity than pure TiO_2. Reactivity of TiO_2 depends on many factors: the adsorption of dye on catalyst surface,[44] band-gap energy, surface area, crystal size, crystallinity, and electron-hole recombination rate,[45-47] therefore an explanation of reactivity order in complicated. The addition of transition metals on the TiO_2 photocatalyst surface can enhance the photocatalytic degradation activity due to the lower crystal size, higher surface area, higher efficiency for the electron hole regeneration, and the charge trapping. The charge trapping can be demonstrated by the following equations. [48]

When transition metal ions replaced Ti ions of TiO_2, most of the dopant levels appeared between the valence band and the conduction band of TiO_2, which can increase the surface trapping rate of carrier and retarded the electron-hole recombination[45] and therefore, the photocatalytic activity of TiO_2 can be enhanced.

The addition of transition metals on the TiO_2 photocatalyst surface can enhance the photocatalytic degradation activity due to the higher efficiency for the electron hole regeneration, and the charge trapping. The charge trapping can be demonstrated by the following equations:

$$TiO_2 + hv \rightarrow e^- cb + h^+ vb \quad (1)$$

$$Fe^{3+} + e^- cb \rightarrow Fe^{2+} \quad (2)$$

$$Fe^{3+} + h^+ vb \rightarrow Fe^{4+} \quad (3)$$

The holes can transfer to the surface of TiO_2 and react with OH- to produce active $OH^{\cdot}$.

When transition iron ions replaced Ti ions of TiO_2, most of the dopant levels appeared between the valence band and the conduction band of TiO_2, which can increase the surface trapping rate of carrier and retarded the electron-hole recombination, so Fe^{3+} can improve the photocatalytic efficiency by enhancing processes such as separation of photogenerated charges (by hole or electron trapping), detrapping and/or transfer of trapped charges to interface and to adsorbed substrates, reducing consequently recombination.

$$I + MB \rightarrow I\text{-}MB \quad (4)$$

(I: adsorption site)

$$I\text{-}MB + OH^{\cdot} \rightarrow I + \text{aliphatic compounds} + OH^{\cdot} \rightarrow CO_2 + H_2O + \text{inorganic} \quad (5)$$

Fullerene had an energy sensitizer effect for improving quantum efficiency and increasing charge transfer.[49] With fullerene amend TiO_2 the surface area increase, and enhance the adsorption of dye on catalyst surface.

The degradation of MB concentration in aqueous solution occurred via the three kinds of physical phenomena: quantum efficiency of the fullerene; organo-metallic reaction of the Fe compound; and decomposition of TiO_2. For these reasons Fe-fullerene/TiO_2 have higher photoactivity than pure TiO_2 and Fe-TiO_2.

4. Conclusion

In this study, we present the preparation and characterization of pure TiO_2, Fe-TiO_2 and Fe-fullerene/TiO_2 composites. These three kinds of photocatalyst were characterized by their structural variations, surface state and photocatalytic by X-ray diffraction (XRD), scanning electron microscopy (SEM), energy dispersive X-ray (EDX) spectroscopy and transmission electron microscope (TEM). In the XRD patterns, the diffraction patterns demonstrated peaks of high crystallinity of anatase. In the SEM image, TiO_2 particles regularly dispersed on the fullerene surface. The EDX spectrum showed the presence of C, O, and Ti, as major elements, with Fe peaks. The absorbance maxima of MB solution decrease with an increase of the UV-light irradiation time. The degradation rate of Fe-fullerene/TiO_2 composites is shown the biggest. According to the degradation results, the decrease of the MB concentration express that TiO_2 was treated by Fe and fullerene can advance the catalytic activity for degradation MB solutions.

Acknowledgement

This work was supported by Research Foundation from Hanseo University in 2009. The authors are grateful to staffs in the University for financial support

References

1. E. Piera, M. I. Tejedor, M. E. Zorn and M. A. Anderson, Appl. Catal. B: Environ., **47**, 219 (2004).
2. Fujishima, K. Hashimoto and T.Watanabe, Inc., May

1999.
3. C. G. Silva, W. Wang and J. L. Faria, J. Photochem. Photobiol. A: Chem., **181**, 314 (2006).
4. V. Shah, P. Verma, P. Stopka, J. Gabriel, P. Baldrian and F. Nerud, Appl. Catal. B: Environ., **46**, 287 (2003).
5. I. K. Konstantinou and T. A. Albanis, Appl. Catal. B: Environ., **42**, 319 (2003).
6. T. Sauer, G. Cesconeto Neto and H. J. Jose, J. Photochem. Photobiol. A: Chem., **149**, 147 (2002).
7. M. R. Hoffmann, S. T. Martin, W. Choi and D. W. Bahnemann, Chem. Rev., **95,** 69 (1995).
8. A. Fujishima, T. N. Rao and D. A. Tryk, J. Photochem. Photobiol., C **1,** 1 (2000).
9. A. L. Linsebigler, G. Lu and J. T. Yates, Chem. Rev., **95,** 735 (1995).
10. H. Tada, M. Yamamoto and S. Ito, Langmuir, **15,** 3699 (1999).
11. M. Gopal, W. J. M. Chan and L. C. De Jonghe, J. Mater. Sci., **32**, 6001 (1997).
12. M. R. Hoffmann, S. T. Martin, W. Y. Choi and D. W. Bahnemann, Chem. Rev., **95**, 69 (1995).
13. C. Minero, G. Marirlla, V. Maurino and E. Pelizzetti, Langmuir, **16**, 2632 (2000).
14. C. Wang, D. F. Bahnemann and J. K. Dohrmann, Chem. Commun., **16**, 1539 (2000).
15. D. Porath, Y. Levi, M. Tarabiah and O. Millo, Phys. Rev., B. **56,** 9829 (1997).
16. V. Brezova, A. Stasko, K. D. Asmus and D. M. Guldi, J. Photochem. Photobiol. A: Chem., **117**, 61 (1998).
17. A. Sclafani, M. N. Mozzanega and P. Pichat, J. Photochem. Photobiol. A: Chem., **59**, 181 (1991).
18. I. M. Arabatzis, T. Stergiopoulos, M. C. Bernard, D. Labou, S. G. Neophytides and P. Falaras, Appl. Catal. B: Environ., **42**, 187 (2003).
19. I. M. Arabatzis, T. Stergiopoulos, D. Andreeva, S. Kitova, S. G. Neophytides and P. Falaras, J. Catal., **220**, 127 (2003).
20. B. Sun, A. V. Vorontsov and P. G. Smirniotis, Langmuir, **19**, 3151 (2003).
21. V. Vamathevan, R. Amal, D. Beydoun, G. Low and S. McEvoy, J. Photochem. Photobiol. A Chem., **148**, 233 (2002).
22. J. Wang, S. Uma and K. J. Klabunde, Appl. Catal.B: Environ., **48**, 151 (2004).
23. B. O'Regan and D. T. Schwartz, J. Appl. Phys., 80, 4749 (1996).
24. C. Wang, C. Bottcher, D. W. Bahnemann and J. K. Dohrmann, J. Mater. Chem., **13**, 2322 (2003).
25. S. Nahar, K. Hasegawa and S. Kagaya, Chemosphere, **65**, 1976 (2006).
26. T. Hasobe, S. Hattori, P. V. Kanmat and S. Fukuzumi, Tetrahedron., **62**, 1937 (2006).
27. B. E. Lawrence, Carbon, **35**, 437 (1997).
28. T. Inoue, Y. Kubozono, K. Hiraoka, K. Mimura, H. Maeda, S. Kashino, S. Emura, T. Uruga and Y. Nakata, J. Synchrotron Radiat., **6**, 779 (1999).
29. C. D. Stevenson, J. R. Noyes and R. Reiter, J. Am. Chem. Soc., **122**, 12905 (2000).
30. W. C. Oh, J. G. Kim, H. Kim, M. L. Chen, K. Zhang, Z. D. Meng and F. J. Zhang , Kor. J. Mater. Res., **19**(11), 569 (2009).
31. F. J. Zhang, M. L. Chen and W. C. Oh, Kor. J. Mater. Res., **18**(11), 583 (2008).
32. K. Zhang, Z. D. Meng and W. C. Oh, Kor. J. Mater. Res., **20**(3), 117 (2010).
33. T. Akiyama, A. Miyazaki, M. Sutoh, I. Ichinose, T. Kunitake and S. Yamada, Colloids Surf., **169**, 137 (2000).
34. T. Hasobe, S. Hattori, P. V. Kanmat and S. Fukuzumi, Tetrahedron., **62**, 1937 (2006).
35. B. E. Lawrence, Carbon, **35**, 437 (1997).
36. B. Sun, M. Li, H. Luo, Z. Shi and Z. Gu, Electrochim. Acta, **47**, 3545 (2002).
37. F. Langa, P. Cruz, J. L. Delgado, E. Espildora, M. J. Gomez-Escalonilla and A. Hoz, J. Mater. Chem., **12**, 2130 (2002).
38. W. C. Oh, A. R. Jung and W. B. Ko, Mater. Sci. Eng.: C., **29**, 1338 (2009).
39. M. Drees, K. Premaratne, W. Graupner and J. R. Heflin, Appl. Phys. Lett., 81, 4607 (2002).
40. A. Smontara, A. M. Tonejc, S. Gradecak, A. Tonejc, A. Bilusicand and J. C. Lasjaunias, Mater. Sci. Eng.: C., **19**, 21 (2002).
41. F. A. Khalid, O. Beffort, U. E. Klotz, B. A. Keller, P. Gasser and S. Vaucher, Acta Mater., **51**, 4575 (2003).
42. Z. N. Gu, L. Zhang, John L. Margrave, Valery A. Davydov, A. V. Rakhmanina, V. Agafonov and V. N. Khabashesku, Carbon, **43**, 2989 (2005).
43. H. Wingkei, C. Y. Jimmy and L. Shuncheng, J. Solid State Chem., **179,** 1171 (2006).
44. S. Y. Mak and D. H. Chen, Dyes Pigments., **61,** 93 (2004).
45. J. C. Colmenares, M. A. Aramend, A. Marinas, J. M. Marinas and F. J. Urbano, Appl. Catal. A: Gen., **306,** 120 (2006).
46. R. J. Tayade, R. G. Kulkarni and R.V. Jasra, Ind. Eng. Chem. Res., **45,** 5231 (2006).
47. C. Jianhua, Y. Maosheng and W. Xiaolin, J. Nanopart. Res., **10**, 163 (2008).
48. W. Choi, A. Termin and M. R. Hoffmann, J. Phys. Chem., **98,** 13669 (1994).
49. W. C. Oh and W. B. Ko, J. Ind. Eng. Chem., **15**, 791 (2009).